

Cite this: DOI: 10.1039/c1an15483d

www.rsc.org/analyst

PAPER

## Coupling corona discharge for ambient extractive ionization mass spectrometry

Bin Hu,<sup>a</sup> Xinglei Zhang,<sup>a</sup> Ming Li,<sup>\*b</sup> Xuejiao Peng,<sup>a</sup> Jing Han,<sup>a</sup> Shuiping Yang,<sup>a</sup> Yongzhong Ouyang<sup>a</sup> and Huanwen Chen<sup>\*a</sup>

Received 10th June 2011, Accepted 22nd August 2011

DOI: 10.1039/c1an15483d

Unlike the extractive electrospray ionization (EESI) technique described elsewhere, a corona discharge instead of electrospray ionization has been utilized to charge a neutral solvent spray under ambient conditions for the generation of highly charged microdroplets, which impact a neutral sample plume for the extractive ionization of the analytes in raw samples without any sample pretreatment. Using the positive ion mode, molecular radical cations were easily generated for the detection of non-polar compounds (*e.g.*, benzene, cyclohexane, *etc.*), while protonated molecular ions of polar compounds (*e.g.*, acetonitrile, acetic ether) were readily produced for the detection. By dispensing the matrix in a relatively large space, this method tolerates highly complex matrices. For a given sample such as lily fragrances, more compounds were detected by the method established here than the EESI technique. An acceptable relative standard deviation (RSD 8.9%,  $n = 11$ ) was obtained for the direct measurement of explosives (10 ppb) in waste water samples. The experimental data demonstrate that this method could simultaneously detect both polar and non-polar analytes with high sensitivity, showing promising applications for the rapid detection of a wide variety of compounds present in complex matrices.

### Introduction

Mass spectrometry (MS) is of increasing interest for trace detection. Analysis throughput of mass spectrometry has been dramatically improved by using ambient ionization techniques.<sup>1–3</sup> Typical ionization techniques including desorption electrospray ionization (DESI),<sup>1–4</sup> direct analysis in real time (DART),<sup>5</sup> surface desorption atmospheric pressure chemical ionization (DAPCI),<sup>6</sup> electrospray-assisted laser desorption ionization (ELDI),<sup>7</sup> dielectric barrier discharge ionization (DBDI),<sup>8</sup> low-temperature plasma probe (LTP),<sup>9</sup> desorption atmospheric pressure photoionization (DAPPI),<sup>10</sup> atmospheric pressure solids analysis probe (ASAP),<sup>11</sup> atmospheric pressure glow discharge desorption ionization (APGDI),<sup>12</sup> laser ablation with electrospray ionization (LAESI),<sup>13</sup> easy ambient sonic spray ionization (EASI),<sup>14</sup> matrix-assisted laser desorption electrospray (MALDESI),<sup>15</sup> surface sampling probe (SSP),<sup>16</sup> plasma-assisted desorption ionization,<sup>17</sup> desorption corona beam ionization,<sup>18</sup> charge-assisted laser desorption ionization,<sup>19</sup> *etc.* are

suitable for the direct desorption ionization of analytes on surfaces under ambient conditions. In addition, liquid samples can be analyzed by fused-droplet electrospray ionization.<sup>20</sup> Samples such as liquids,<sup>21</sup> aerosols<sup>22</sup> and even viscous heterogeneous mixtures<sup>23</sup> can be continuously analyzed by extractive electrospray ionization mass spectrometry (EESI-MS) without sample pretreatment. Since the complex matrices are dispensed in a relatively large 3-D space,<sup>24</sup> EESI tolerates complex matrices for trace detection.<sup>25</sup> This feature renders a long-term stability of EESI-MS for the real-time online analysis of raw samples.<sup>26</sup> By keeping the sample spray away from a high voltage, EESI has been demonstrated to be a soft method of transferring protein molecules such as myoglobin, lysozyme, *etc.* into the gas phase without significant conformation change.<sup>27</sup> This extends the application of EESI for the rapid detection of biological molecules in their native forms.

However, the nature of ESI introduces difficulty for ESI-derived techniques (such as DESI, EESI) to sensitively detect compounds of low polarity and/or low proton affinity. Although the detection of some low polar chemicals such as sulfur species is possible using selective ion/molecule reactions,<sup>22</sup> it is highly desirable to measure them in a straight-forward way. It is well known that ambient corona discharge possesses a much higher ionization efficiency than ESI. This accounts for the observation that the sensitivity of corona discharge-based ambient ionization technique (*e.g.*, DAPCI) is normally higher than that of the

<sup>a</sup>Jiangxi Key Laboratory for Mass Spectrometry and Instrumentation, College of Chemistry, Biology and Material Sciences, East China Institute of Technology, Nanchang, Jiangxi Province 330013, P. R. China. E-mail: chw8868@gmail.com; Fax: (+86)-791-3896-370; Tel: (+86)-791-3896-370

<sup>b</sup>National Institute of Metrology, Beijing 100013, P. R. China. E-mail: mingutah@hotmail.com; Tel: (+86)-10-64526353

electrospray-based ambient ionization technique (*e.g.*, EESI) in the case of analyzing small molecules.<sup>28,29</sup> Therefore, coupling ambient corona discharge to extractive ionization may result in a technique with overall analytical performance superior to the normal EESI,<sup>22,26,27</sup> especially for detecting compounds of low proton affinity (PA) and/or low/no polarity. Therefore, an ambient corona discharge rather than an ESI has been employed to produce the primary ionic reagents, which are then utilized for extractive ionization of a wide variety of analytes including both polar and non-polar compounds in a complex matrix.

## Experimental

### Experimental setup

All experiments were carried out on a commercial linear ion trap mass spectrometer (LTQ-XL, Finnigan, San Jose, CA) installed with a home-made corona discharge-assisted extractive ionization source (schematically shown in Fig. 1). Briefly, a high voltage ( $\pm 3.0$  kV) was applied to the tip (radius *ca.* 0.0075 mm) of a stainless steel needle (od: 0.15 mm) to create corona discharge at ambient pressure. Nitrogen with a purity of 99.9999% was used as the nebulizing gas with a flow rate of 3.2 L s<sup>-1</sup> (1.8 MPa). A discharging solution (*e.g.*, methanol/water/acetic acid (50 : 48 : 2, v : v : v), pure water, methanol, *etc.*) was introduced through a fused silica capillary (id: 0.15 mm, od: 0.17 mm) of channel I, with an infusion rate of 5  $\mu$ L min<sup>-1</sup>. Microdroplets formed in the nebulized solvent spray were charged by the corona discharge, producing the highly charged microdroplets. Those charged microdroplets then intersected the neutral sample plume generated by spraying the sample solution or introduced by nitrogen gas flow (channel II). Liquid extraction<sup>25</sup> and charge transfer occurred between the charged and neutral microdroplets, which came from the corona discharge tip and sample spray channel, respectively. The extractive ionization was primarily completed in the spatial cross-section formed between the charged droplet plume, the sample spray plume and the entrance of the LTQ instrument. The ions were then guided into the ion trap for mass analysis. Depending on the analytes

detected, the source assembly was placed at 10 mm (*a*) away from the MS inlet. The angle ( $\gamma$ ) formed between the discharge electrode and channel I was set at 80°. The distance (*b*) between the outlet of channel I and the entrance of the LTQ instrument was set to 10 mm. The angle ( $\beta$ ) formed between the discharge electrode and the ion entrance capillary was set at 80°. The angle ( $\alpha$ ) by channel II against channel I was 60°. The temperature of the heated capillary of the LTQ instrument was maintained at 200 °C. The parameters given here were selected by optimizing the signals of benzene. Values of the voltages for the entrance capillary, ion guide systems, detectors, *etc.* were set at default values without optimization.

### Materials and reagents

Benzene (A. R. Grade), naphthalene (A. R. Grade), cyclohexane (A. R. Grade), acetonitrile (A. R. Grade) were bought from Sinopharm Chemical Reagent Co., Ltd (Shanghai, China); 1,3,5-trinitrobenzene (TNB) was bought from Dr Ehrenstorfer GmbH (Augsburg, Germany); trinitrotoluene (TNT) was bought from Chem Service, Inc. (PA, USA). The deionized water (18.2 M $\Omega$ ·cm) used was prepared with Milli-Q. Fresh lily flower was bought in a local flower market and used directly without any pretreatment. The urine sample was collected from a 26 year-old healthy male volunteer.

### Statement

The present study was approved by the ethics committee of the Institute and adhered to the tenets of the Declaration of Helsinki. Additionally, the written informed consent was obtained from the volunteer and patients.

### Experimental procedures

The mass spectrum was recorded by the Xcalibur<sup>®</sup> software followed by background subtraction. Each mass spectrum was recorded in 1 min and the average is output, unless indicated specifically. For tandem mass spectrometry, the precursor ions of interest were isolated with a window width of 1.4 Da, and then subjected to collision-induced dissociation (CID) experiments performed with 10~45 units (arbitrary units defined by the LTQ instrument) of collision energy (CE) and a duration time of 30 ms.

The gas samples of benzene, cyclohexane, and naphthalene with the concentration of 10 ppb were introduced by the nitrogen gas flow with the flow rate of 5.0 L min<sup>-1</sup>. The gas samples of acetonitrile, acetone, acetic ether, and diethyl ether with the concentration of 100 ppb were introduced in the nitrogen gas flow with the flow rate of 5.0 L min<sup>-1</sup>.

The lily flower fragrance was sampled by using a neutral desorption (ND) device, which was previously described elsewhere.<sup>30</sup> The mixture of the volatile organic compounds (VOCs) of lily and ambient air (relative humidity ~60%) was directly introduced to the charged droplet plume using a Teflon tube (id, 5.0 mm, length, 6 m) with an outlet (id, 1.0 mm), such that the analytes were ionized by either corona discharge or ESI, without any further treatment.

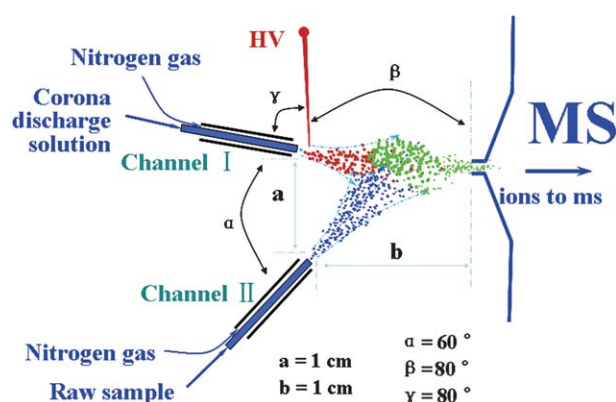


**Fig. 1** Schematic diagram of the ionization source setup. The neutral microdroplets generated by spraying solvent are efficiently charged by the ambient corona discharge, providing more primary ionic species for the ionization of analytes in the sample plume created by neutrally spraying the raw sample solution. Note that the scheme is not proportionally scaled.

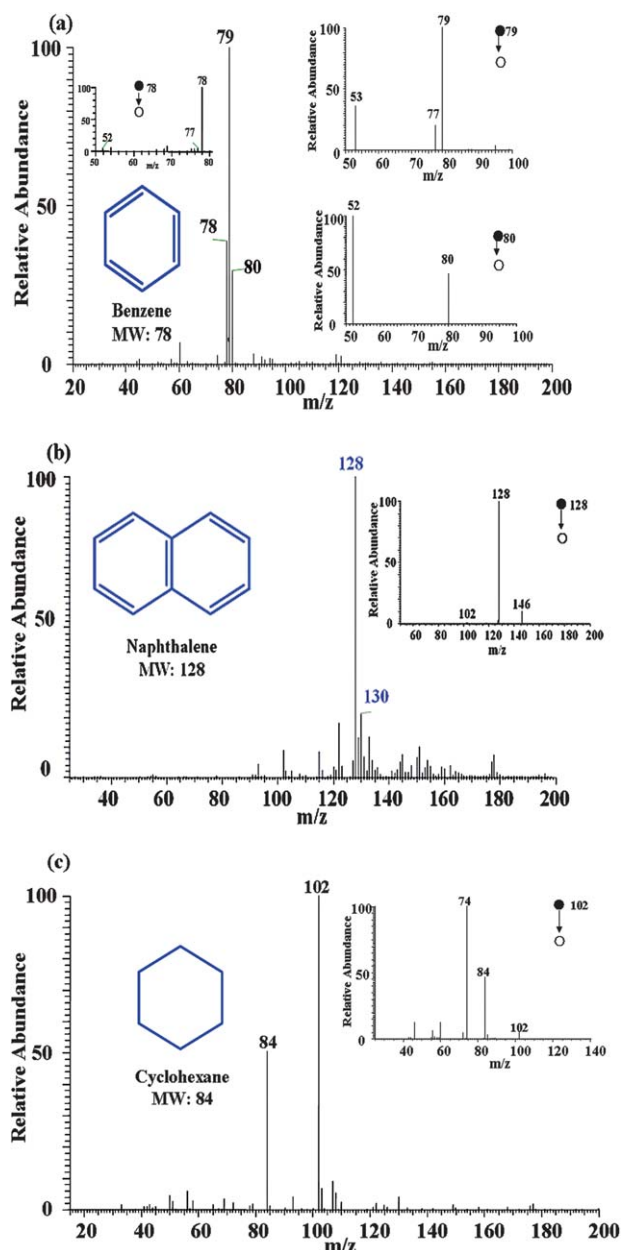


**Fig. 2** Corona discharge-assisted extractive ionization mass spectra of typical non-polar compounds. (a) MS spectrum of benzene, showing 3 characteristic signals at  $m/z$  78, 79 and 80; the insets show the CID spectra of interested ions. (b) MS spectrum of naphthalene; the inset shows the CID spectrum of  $m/z$  128. (c) MS spectrum of cyclohexane; the inset shows the CID spectrum of  $m/z$  102.

## Results and discussion

### Detection of non-polar compounds

Non-polar compounds are normally undetectable using ESI or its variant techniques such as EESI. As the first trial, benzene (MW 78), a typical non-polar compound and an environment pollutant of wide interest, was analyzed. Interestingly, benzene was detected at  $m/z$  78, 79 and 80 (Fig. 2), which were ascribed to the benzene radical cations ( $m/z$  78), protonated benzene ( $m/z$  79) and the resultant radical cations ( $m/z$  80) generated through

Birch reduction of benzene,<sup>31</sup> respectively. Upon CID, the benzene radical cations ( $m/z$  78) gave a small peak at  $m/z$  77 and a major peak at  $m/z$  52 (Fig. 2a), by the loss of H and  $C_2H_2$ , respectively. These observations are in good agreement with the previous results obtained using APCI-MS.<sup>32</sup> Under the CID conditions, the protonated benzene ( $m/z$  79), which might result from self-ionization of benzene inside the ion trap, cleaved 2H and  $C_2H_2$  to yield ions of  $m/z$  77 and  $m/z$  53 (inset of Fig. 2a), respectively. The ions of  $m/z$  80 were also observed in the LTP experiment, where cyclohexadiene was produced *via* ambient Birch reduction.<sup>31</sup> In this study, the precursor ions of  $m/z$  80 generated a predominant peak at  $m/z$  52 (inset of Fig. 2a), probably by the loss of  $C_2H_4$ . The  $C_2H_2$  was cleaved from either  $m/z$  79 or  $m/z$  78 ions while the neutral loss of  $C_2H_4$  from the ions of  $m/z$  80 was observed under the CID processes, indicating that the residue ions (*i.e.*,  $m/z$  53,  $m/z$  52) have similar structures and the 2 hydrogen atoms were added to 2 neighboring carbon atoms of the benzene ring during the Birch reaction. These fragmentations provide the characteristic evidences confirming the detection of benzene. Usually, benzene is detected as radical cations at  $m/z$  78 using APCI-MS,<sup>32,33</sup> while the signals at  $m/z$  79 or 80 are rarely detected using APCI-MS.<sup>32</sup> The simultaneous observation of benzene signals at  $m/z$  78, 79 and  $m/z$  80 means that the mechanism of the corona discharge-assisted extractive ionization differs from that of typical EESI or APCI, because ESI has no capability to directly ionize the non-polar species and APCI forms no ionic benzene species of  $m/z$  79 and  $m/z$  80.

Under the same conditions, typical non-polar compounds such as naphthalene (MW 128) and cyclohexane (MW 84) were also successfully ionized by the corona discharge-assisted extractive ionization technique. Similar to benzene, naphthalene radical cations at  $m/z$  128 and ionic resultant of Birch reduction ( $m/z$  130) with low intensity were observed (Fig. 2b). During the CID process, naphthalene radical cation  $m/z$  128 yielded a peak at  $m/z$  146 (inset of Fig. 2b) with significant abundance. This peak was ascribed to the radical cations of naphthalene water adduct  $[M + H_2O]^+$ , which was generated by reacting with water vapor inside the ion trap. The water cluster exclusively created the naphthalene radical cations ( $m/z$  128) in the MS<sup>3</sup> spectrum (not shown). A small peak at  $m/z$  102 was also observed in the CID spectrum (inset of Fig. 2b), probably by the loss of  $C_2H_2$ . This peak is of relatively low abundance, representing that this fragmentation pathway is not favored under these conditions. The cyclohexane was detected at abundant peaks of  $m/z$  84 and  $m/z$  102, which corresponded to the cyclohexane radical cations  $[M]^+$  and the radical cations of cyclohexane water adducts  $[M + H_2O]^+$  (Fig. 2c), respectively. The water adducts ( $m/z$  102) cleaved water to yield cyclohexane radical cations of  $m/z$  84 when a low collision energy ( $\leq 10\%$ ) was applied to the CID experiments; more fragments of  $m/z$  74, 60 and  $m/z$  46 were also detected (inset of Fig. 2c) when high collision energy ( $> 20\%$ ) was used. These ions are probably responsible for the loss of  $CH_2=CH_2$ ,  $CH_2=CH-CH_3$ , and  $2CH_2=CH_2$ , respectively. More interestingly, the intensity of the radical cations of the cyclohexane water adduct ( $m/z$  102) is much higher than that of the cyclohexane radical cations ( $m/z$  84), showing a useful hint that the water molecules may stabilize the molecule radical cations.

**Table 1** Summary of the data obtained using corona discharge-assisted extractive ionization MS

Compounds (MW)	Proton affinity/kJ mol <sup>-1</sup> <sup>a</sup>	Ionization energy/eV <sup>b</sup>	Observed ions		
			Ionic species	Signals ( <i>m/z</i> )	Major fragments (MS/MS) ( <i>m/z</i> )
Benzene (78)	750.4	9.25	[M] <sup>+</sup> , [M + H] <sup>+</sup> , [M + 2H] <sup>+</sup>	78, 79, <sup>c</sup> 80	53
Toluene (92)	784	8.82	[M] <sup>+</sup> , [M + 2H] <sup>+</sup>	80, 92, 94 <sup>c</sup>	78
Cyclohexane (84)	686.9	9.86	[M] <sup>+</sup> , [M + H <sub>2</sub> O] <sup>+</sup>	84, 102 <sup>c</sup>	84
Naphthalene (128)	802.9	8.14	[M] <sup>+</sup> , [M + 2H] <sup>+</sup>	128, <sup>c</sup> 130	146
Acetonitrile (41)	779.2	12.19	[M + H] <sup>+</sup> , [M + H <sub>2</sub> O + H] <sup>+</sup>	42, 59 <sup>c</sup>	42, 55
Acetone (58)	812	9.71	[M + H] <sup>+</sup> , [M + H <sub>2</sub> O] <sup>+</sup>	59, 76 <sup>c</sup>	43, 58
Acetic ether (88)	827.3	10.01	[M + H] <sup>+</sup> , [M + H <sub>2</sub> O] <sup>+</sup>	89, <sup>c</sup> 106	61
Diethyl ether (74)	828.4	9.51	[M + H] <sup>+</sup> , [M + H <sub>2</sub> O] <sup>+</sup>	75, <sup>c</sup> 92	47
Water (18)	691.0	12.61	[2M] <sup>+</sup> , [2M + H] <sup>+</sup>	36, 37 <sup>c</sup>	19
Methanol (32)	754.3	10.85	[M] <sup>+</sup> , [M + H] <sup>+</sup> , [2M + H] <sup>+</sup>	32, 33, 65 <sup>c</sup>	33

<sup>a</sup> Ref: E. P. L. Hunter and S. G. Lias, *J. Phys. Chem. Ref. Data*, 1998, **27**, 413–656. <sup>b</sup> Ref: S. G. Lias, J. E. Bartmess, J. F. Liebman, J. L. Holmes, R. D. Levin and W. G. Mallard, *J. Phys. Chem. Ref. Data*, 1988, **17**(suppl. 1) 1–861. <sup>c</sup> The precursor ions selected for CID experiments.

### Detection of weakly polar compounds

In EESI, weakly polar analytes are poorly protonated, and thus require specific ion/molecule reactions to improve the sensitivity of the detection. Using the method reported here, weakly polar compounds including acetonitrile, acetone, acetic ether, and diethyl ether were detected and the ionic fragments observed in the MS/MS experiments are summarized in Table 1. For instance, acetonitrile (MW 41) gave abundant signals at *m/z* 42, 59 and *m/z* 83 (Fig. 3a), which were ascribed to the protonated acetonitrile [M + H]<sup>+</sup>, the radical cations of the acetonitrile water adducts [M + H<sub>2</sub>O]<sup>+</sup> and the proton-bound acetonitrile dimers [2M + H]<sup>+</sup>, respectively. Upon CID, the precursor ions of *m/z* 83 dissociated into ionic fragments of *m/z* 55 and *m/z* 42, by the loss of C<sub>2</sub>H<sub>4</sub> (or 2CH<sub>2</sub>)<sup>34</sup> and acetonitrile, respectively. The water adducts (*m/z* 59) generated acetonitrile radical cations (*m/z* 41) by the loss of water. This finding is consistent with the fact that the ionization energy (IE) of water (12.61 eV) is higher than that of acetonitrile (12.19 eV). Compounds such as diethyl ether (MW 74) and acetic ether (MW 88) were also detected in a similar way. As shown in Fig. 3b, the abundant peaks appeared at *m/z* 75, *m/z* 92 and *m/z* 149 were generated due to the protonated diethyl ether [M + H]<sup>+</sup>, the water adducts [M + H<sub>2</sub>O]<sup>+</sup> and protonated dimer [2M + H]<sup>+</sup>, respectively. During the CID process, the protonated diethyl ether molecular ions (*m/z* 75) generated fragments of *m/z* 59 and *m/z* 61 (inset of Fig. 3b) probably by the loss of CH<sub>2</sub> and CH<sub>4</sub> (or, 2H + CH<sub>2</sub>),<sup>35</sup> respectively. The protonated dimer (*m/z* 149) lost water, CH<sub>2</sub>CH<sub>2</sub> and a neutral diethyl ether molecule to yield the fragments of *m/z* 131, *m/z* 121 and *m/z* 75 (inset of Fig. 3b), respectively. As shown in Fig. 3c, the abundant peaks appeared at *m/z* 89, *m/z* 106 and *m/z* 177 were assigned to the protonated acetic ether [M + H]<sup>+</sup>, the water adducts [M + H<sub>2</sub>O]<sup>+</sup> and the proton-bound acetic ether dimer [2M + H]<sup>+</sup>, respectively. The protonated acetic ether (*m/z* 89) created an abundant peak at *m/z* 61 by the loss of CO (inset of Fig. 3c) during the CID process. The radical cations of acetic ether water adducts (*m/z* 106) produced major peaks at *m/z* 88, *m/z* 89 and *m/z* 64 by the loss of H<sub>2</sub>O, OH and CH<sub>2</sub>CO (inset of Fig. 3c), respectively. The proton-bound acetic ether dimer mainly dissociated into protonated acetic ether, showing a predominant peak at *m/z* 89 in the CID spectrum (inset of Fig. 3c).

When a 10 ppb solution of TNT in methanol was introduced to the corona discharge-assisted extractive ionization source operated in the negative ion detection mode, the signals of TNT were detected at *m/z* 227 and *m/z* 226 (Fig. 4a), which were ascribed to the TNT radical anions (*m/z* 227) and the deprotonated TNT molecules (*m/z* 226), respectively. Upon CID, the TNT radical anions (*m/z* 227) generated major fragments of *m/z* 212, *m/z* 197 and *m/z* 183 by the loss of CH<sub>3</sub>, NO and CH<sub>2</sub>NO, respectively. The fragmentation pathway is in good agreement with the previously reported data.<sup>36</sup> The deprotonated TNT (*m/z* 226) underwent less intensive fragmentation, and produced a predominant peak at *m/z* 196, by the loss of NO.<sup>36</sup> On the other hand, only TNT radical anions (*m/z* 227) were detected as the base peak (Fig. 4b) when the same TNT solution was introduced to a normal EESI source. The observation of deprotonated TNT suggests that the internal energy of the TNT anions created by this method is considerably higher than that of the ions created by the EESI technique. This is in agreement with the conclusion that electrospray-based ambient ionization techniques are generally gentler than corona discharge-based techniques as depicted in ref. 29. This indicates that the corona discharge-assisted extractive ionization works in the mechanism differing from that of EESI because the primary ions from these two techniques are different.

### Ionization mechanism

Both non-polar compounds and polar compounds can be detected by the technique reported here. As shown in Table 1, the signal formation was largely dependent on the proton affinity (PA) and the ionization energy (IE) values of the analytes. If the IE of the analyte is relatively higher and the PA of the analyte is not lower than that of water (691.0 kJ mol<sup>-1</sup>), the analyte is likely to be protonated or to form radical cations of water adduct [M + H<sub>2</sub>O]<sup>+</sup>. Acetonitrile (PA 779.2 kJ mol<sup>-1</sup>, IE 12.19 eV) shows an example for this case. If the IE of the analyte is significantly lower than that of water, the analyte most likely forms radical cations M<sup>+</sup>. The non-polar compounds such as toluene, cyclohexane and naphthalene are the examples tested in this study. Note that naphthalene has a high PA (802.9 kJ mol<sup>-1</sup>), but it gives radical cations rather than the protonated molecules, probably because naphthalene has a low IE and no suitable site

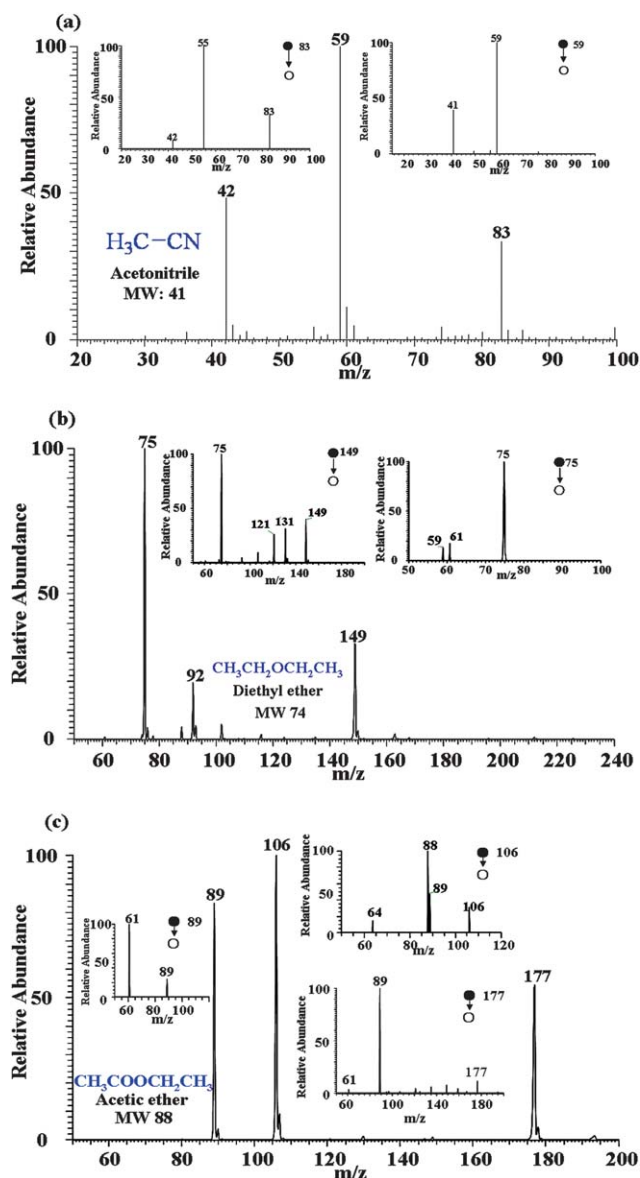


**Fig. 3** Corona discharge-assisted extractive ionization mass spectra of weakly polar compounds. (a) MS spectrum of acetonitrile; the insets show the CID spectra of interested ions. (b) MS spectrum of diethyl ether, the insets show the fragments obtained in the CID experiments. (c) MS spectrum of acetic ether, the insets show the fragments obtained in the CID experiments. Note that water was used as the discharging solution for collecting these MS spectra.

to accept the proton. For the analytes which have possible sites for protonation, the analytes are apt to be protonated even if the IE values of the analytes are lower than that of water. Acetone, acetic ether, diethyl ether and methanol are the representative examples in this study. Benzene was detected by forming protonated molecular ions and radical cations, probably because it has a medium-levelled PA ( $750.4 \text{ kJ mol}^{-1}$ ) and IE (IE  $9.25 \text{ eV}$ ) values. Our preliminary data show that the ion production is heavily related to the unique process of ambient corona discharge, which probably produces energetic species such as water radical cations, nitrogen radical cations, *etc.* These active radical cations are likely to be involved in the ionization of

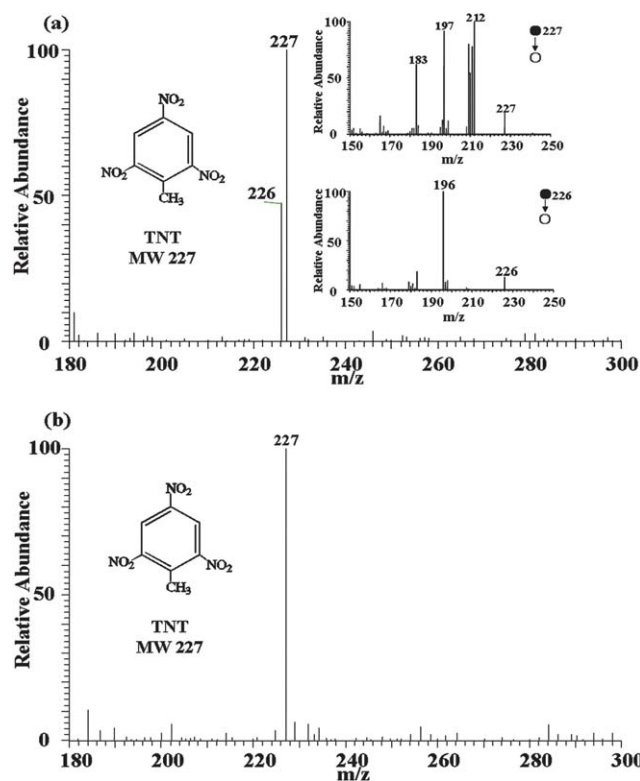


**Fig. 4** Comparison with corona charge-assisted extractive ionization and EESI for the detection of TNT. (a) Both TNT radical cations ( $m/z$  227) and deprotonated molecules of TNT ( $m/z$  226) detected using corona discharge-assisted extractive ionization MS; the insets show the MS/MS of ions at  $m/z$  226 and  $m/z$  227. (b) Typical mass spectrum recorded using EESI-MS; only TNT radical anions ( $m/z$  227) were detected.

compounds with low polarities. The detailed mechanism required further studies, and progress is underway.

### Matrix tolerance

Analogous to the previously reported EESI techniques,<sup>21,22,26,37,38</sup> the corona discharge-assisted extractive ionization also tolerates complex matrices for trace analysis. For example, weakly polar TNB (MW 213) in waste water (10 ppb), which was taken from a waste pool of a local painting plant, was detected in negative ion detection mode, giving a peak at  $m/z$  213, which corresponded to the radical anions. During the CID experiments, as shown in Fig. 5a, the radical anions of TNB ( $m/z$  213) produced major fragments of  $m/z$  183,  $m/z$  197 and  $m/z$  167 by the loss of NO, O and NO<sub>2</sub> (inset of Fig. 5a), respectively. These fragments have been observed using negative DAPCI,<sup>36</sup> which is also a corona discharge-based technique. Note that TNB was only detected *via* ion/molecular reaction using normal EESI-MS.<sup>39</sup> The direct detection of TNB in complex matrices shows the attractive aspects of the corona discharge-assisted extractive ionization for rapid trace analysis.

Urine analysis has also been of increasing interest in recent years. To challenge the corona discharge-assisted extractive ionization technique, a raw urine sample spiked with 1 ppb benzene was directly sprayed into the source without any matrix cleaning. Dominant peaks appeared at  $m/z$  61, 121, 163, 181, 212,

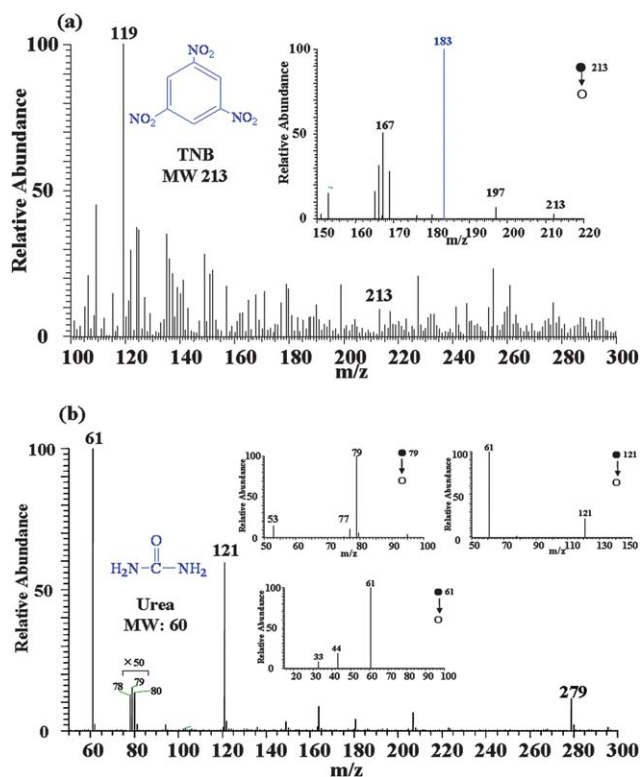


**Fig. 5** MS spectra of complex samples. (a) Mass spectrum of TNB in the waste water sample in the negative ion detection mode; the insets show the fragments obtained in the CID experiments. (b) MS spectrum of a urine sample spiked with trace benzene (1 ppb); the characteristic fragments observed in the CID experiments which detect both non-polar (such as benzene) and polar compounds (such as urea, *etc.*) in the complex urine sample.

279, *etc.*, and the typical benzene signals ( $m/z$  78, 79 and  $m/z$  80) were detected simultaneously in the mass spectrum (Fig. 5b). Upon CID, the fragmentation patterns of the benzene signals were in accordance with those observed using the benzene sample without complex matrices. For example, the CID spectrum of the protonated benzene molecules shows major peaks at  $m/z$  77 and  $m/z$  53 (inset of Fig. 5b), generated by the loss of 2H and  $C_2H_2$ , respectively. The base peak at  $m/z$  61 and the peak at  $m/z$  121 were ascribed to the protonated urea and the proton-bound urea dimer, respectively. The proton-bound urea dimer ( $m/z$  121) cleaved neutral urea when subjected to CID (inset of Fig. 5b); and the precursor ions ( $m/z$  61) could lose  $NH_3$  and CO to generate ions of  $m/z$  44 and  $m/z$  33 (inset of Fig. 5b), respectively. These data show that the technique reported here is able to directly analyze complex samples such as urine or waste water without matrix separation.

Since the corona discharge-assisted extractive ionization technique tolerates complex matrices, it may detect more ingredients when an actually unknown sample is analyzed. This feature is especially attractive for 'omics' studies. As a demonstration, the fragrance of a fresh lily sampled by neutral desorption sampling<sup>30,39,40</sup> was used as the unknown sample. A mass spectral fingerprint of lily fragrance using corona discharge-assisted extractive ionization (Fig. 6b) shows many more signals than that detected by using normal EESI (Fig. 6a).

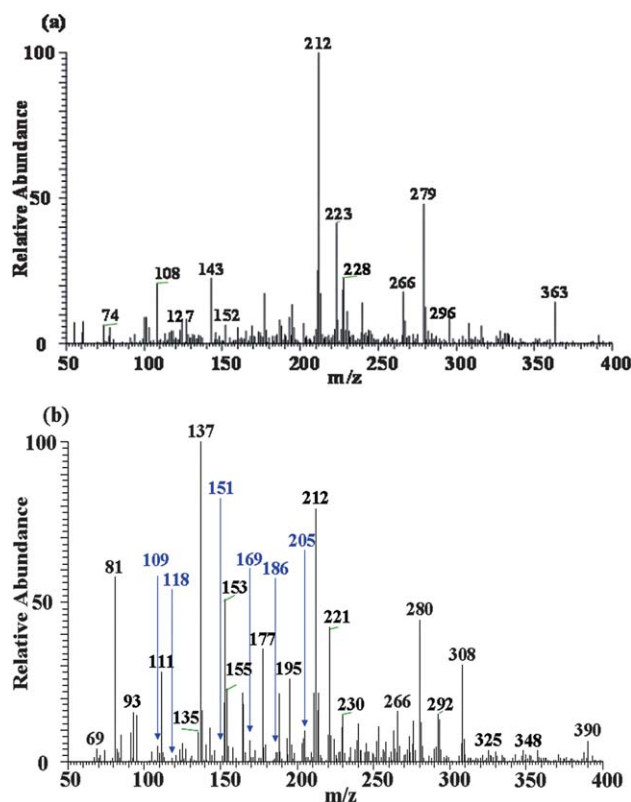


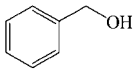
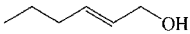
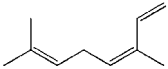
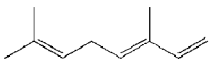
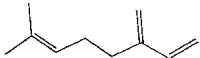
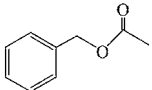
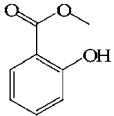
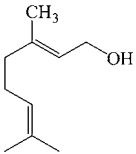
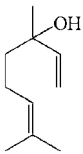
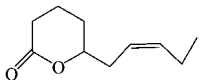
**Fig. 6** More compounds detected by corona discharge-assisted extractive ionization than EESI from the lily fragrance: (a) the fingerprint of lily recorded using EESI; (b) the fingerprint of lily recorded using corona discharge extractive ionization.

The peaks at  $m/z$  109, 118, 137, 151, 153, 169 and 172 are corresponding to the protonated or hydration molecules of benzyl alcohol,<sup>41</sup> hexenol,<sup>41</sup> ocimene (and/or  $\beta$ -myrcene),<sup>41–43</sup> benzyl acetate,<sup>41</sup> methyl salicylate,<sup>41</sup> jasmine lactone,<sup>41,43</sup> and geraniol,<sup>42</sup> respectively. The aim of this study is to show the ionization ability for the non-polar and weakly polar compounds with complex matrices and the discrimination of the isomers is beyond of this study. The probable molecular structures of these compounds were speculated by CID and the fragment ions are listed in Table 2. The peaks such as at  $m/z$  69, 81, 93, 111, 177, and 195 were unknown at this stage, but they could be identified using multiple stage mass spectrometry or high resolution mass spectrometry. Meanwhile, the signals undetectable by EESI are also marked in Table 2, showing that more peaks can be detected by the corona discharge-assisted extractive ionization when complex samples such as the lily fragrance are analyzed.

### Quantitative analysis

Quantitative analysis of TNB in the waste water samples was performed for the evaluation of the performance of this new technique. The product ions of  $m/z$  183 in MS/MS spectra were selected for the quantitative analysis. As the result, the dynamic response range of 4 orders of magnitude in the logarithmic scales was obtained (Fig. 7a). The signal response was represented by the equation  $\lg I = 0.1539 \lg C (\text{g mL}^{-1}) + 2.6407$ ,  $R^2 = 0.997$ . This equation also shows that the signal responded as a power

**Table 2** Compounds found in the lily fragrance using corona discharge-assisted extractive ionization MS/MS

Compounds	Molecular structure	Molecular weight	Observed ions		Main product ions <i>m/z</i> (relative intensity) and corresponding neutral loss
			Ionic species	<i>m/z</i>	
Benzyl alcohol <sup>a</sup>		108	[M + H] <sup>+</sup>	109	91 (100) H <sub>2</sub> O, 67 (45) CH <sub>2</sub> CO
Hexenol <sup>a</sup>		100	[M + H <sub>2</sub> O] <sup>+</sup>	118	100 (100) H <sub>2</sub> O, 90 (30) CO, 82 (25) 2H <sub>2</sub> O, 72 (35) CH <sub>3</sub> CH <sub>2</sub> OH
<i>cis</i> -Ocimene <sup>a</sup>					
<i>trans</i> -Ocimene <sup>a</sup>		136	[M + H] <sup>+</sup>	137	109 (20) C <sub>2</sub> H <sub>2</sub> , 95 (100) CH <sub>3</sub> CH=CH <sub>2</sub> , 81 (60) CH <sub>3</sub> CH <sub>2</sub> CH=CH <sub>2</sub> , 57 (20) CH≡CCH=CH=C(CH <sub>3</sub> ) <sub>2</sub>
β-Myrcene <sup>a</sup>					
Benzyl acetate		150	[M + H] <sup>+</sup>	151	133 (70) H <sub>2</sub> O, 107 (100) CO <sub>2</sub> , 91 (15) CH <sub>3</sub> COOH
Methyl salicylate		152	[M + H] <sup>+</sup>	153	135 (100) H <sub>2</sub> O, 109 (35) CO <sub>2</sub> , 121 (15) CH <sub>3</sub> OH
Geraniol		154	[M + H] <sup>+</sup>	155	137 (100) H <sub>2</sub> O, 109 (60) CH <sub>3</sub> CH <sub>2</sub> OH, 95 (40) CH <sub>3</sub> CH <sub>2</sub> OH, 85 (20) CH <sub>3</sub> CH=C(CH <sub>3</sub> ) <sub>2</sub>
Linalool					
Jasmine lactone		168	[M + H] <sup>+</sup> [M + H <sub>2</sub> O] <sup>+</sup>	169 186	154 (20) CH <sub>3</sub> , 151 (100) H <sub>2</sub> O, 141 (30) CO 171 (100) CH <sub>3</sub> , 158 (95) CO, 142 (30) CO <sub>2</sub> , 130 (20) CH <sub>3</sub> CH <sub>2</sub> CH=CH <sub>2</sub>

<sup>a</sup> The signals were undetectable by EESI-MS.

function of the concentration levels of the analytes. The non-linear dynamic range observed for the analyte detection resulted from the molecular interactions of the charged species and the neutral molecules. This non-linear response curve indicates that the analyte signals were generated by a complicated process, in which the analyte signal increased slowly along with its concentration levels. Note that  $R^2$  is 0.997 in the logarithmic scales, showing that the responses strictly followed the power function and thus enabling quantitative detection. These findings suggest that although the signal levels were quantitatively increased with

the analyte levels the ionization process differed from commonly observed cases such as ESI, DESI, where the signal levels increased proportionally with the concentration levels of the analytes.<sup>44,45</sup> This was also observed for detection of urinary benzene (see below), but the detailed mechanism remained for further studies. The LOD for the detection of TNB was estimated to be 12 pg ( $S/N = 3$ ), and the RSD was 8.9% ( $n = 11$ ).

As urinary benzene can be used as a chemical marker of benzene exposure,<sup>46,47</sup> it is highly desirable to measure benzene levels in raw urine samples. Although benzene vapor in air

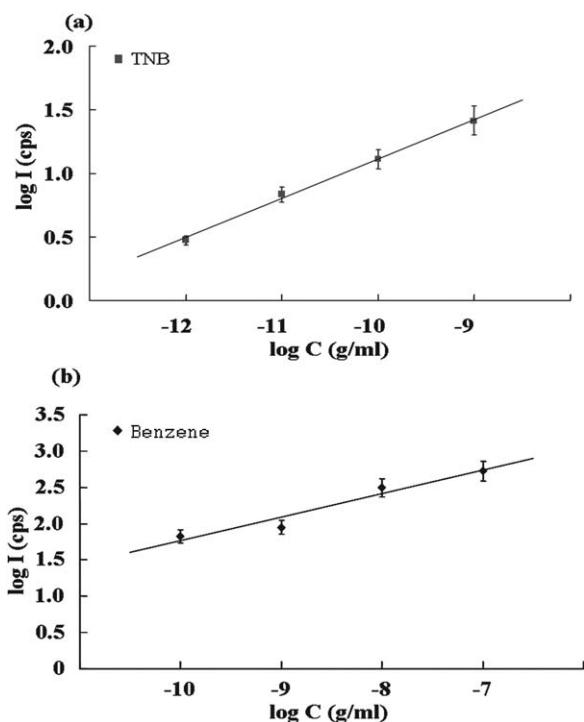


**Fig. 7** The dynamic range of signal responses obtained using corona discharge-assisted extractive ionization mass spectrometry: (a) signal response of TNB ( $m/z$  183) obtained using the characteristic fragment; (b) signal responses of benzene plots of the signal abundances of the fragment ( $m/z$  79) obtained in vs. sample concentration. The error bar is the standard deviation ( $n = 3$ ).

samples can be detected using APCI-MS,<sup>32,33</sup> it is difficult to directly detect trace benzene in aqueous samples using EESI-MS. As demonstrated here, the corona discharge-assisted extractive ionization technique detected trace levels of benzene (1 ppb) spiked into an undiluted human urine sample, showing the typical benzene signals of  $m/z$  78, 79 and  $m/z$  80 (Fig. 5b). Note that the benzene ions were confirmed by their MS/MS data, which were in good agreement with those obtained using benzene solutions without urine matrix. The signal responses of benzene ( $m/z$  79) are shown in Fig. 7b, with a dynamic range of 4 orders of magnitude in the logarithmic scales. The signal response is also described by the equation  $\lg I = 0.1281 \lg C (\text{g mL}^{-1}) + 2.0635$ ,  $R^2 = 0.95$ . The signal levels of benzene maintained constant for more than 5 h when the raw human urine sample was continuously infused, showing a long-term stability comparable to EESI.<sup>19</sup>

## Conclusions

Ambient corona discharge, instead of a high voltage ESI, has been used to efficiently produce highly charged microdroplets, which are then directed for extractive ionization of analytes in the sample plume generated by neutrally spraying the liquid sample. Compared to the conventional APCI, the technique developed in this study can be used for the direct analysis of samples with complex matrix, requiring no sample pretreatment. Although DAPCI tolerates heavy matrices, non-polar compounds cannot be readily ionized using DAPCI. By contrast,

the technique reported here enables the sensitive detection of compounds of a wide variety of polarity, including non-polar analytes, weakly polar molecules and polar chemicals. The non-polar/weakly polar compounds, which are not detectable using EESI or ESI, are easily detected by this method. The experimental data showed that the internal energy of the ions produced by this method differed from those generated by EESI, indicating that the mechanism of the corona discharge-assisted extractive ionization should be different from that of EESI. By dispensing the matrix in a relatively wide spatial section, the untreated raw samples (e.g., urine and waste water sample) can be continuously monitored without significant signal loss. The analytes of interest were identified using tandem mass spectrometry, and the quantitative measurement of trace analytes was completed by using the characteristic fragments obtained in the tandem mass spectrometry experiments. The dynamic signal response range was about 4 orders of magnitude, with detection limits at ppb levels. These features make the corona-assisted extractive ionization attractive for applications in multiple disciplines such as petroleum analysis, natural product detection, drug discovery, and environment analysis.

## Acknowledgements

This work was supported by the Innovation Method Fund of China (2008IM040400), National Natural Science Foundation of China (No. 21005024, 20827007).

## References

- 1 R. G. Cooks, Z. Ouyang, Z. Takats and J. M. Wiseman, *Science*, 2006, **311**, 1566–1570.
- 2 Z. Ouyang and X. Zhang, *Analyst*, 2010, **135**, 659–660.
- 3 Z. Takats, J. M. Wiseman, B. Gologan and R. G. Cooks, *Science*, 2004, **306**, 471–473.
- 4 G. Paglia, D. R. Iffa, C. Wu, G. Corso and R. G. Cooks, *Anal. Chem.*, 2010, **82**, 1744–1750.
- 5 R. B. Cody, J. A. Laramée and H. D. Durst, *Anal. Chem.*, 2005, **77**, 2297–2302.
- 6 S. Yang, J. Ding, J. Zheng, B. Hu, J. Li, H. Chen, Z. Zhou and X. Qiao, *Anal. Chem.*, 2009, **81**, 2426–2436.
- 7 J. Shiea, C. Yuan, M. Huang, S. Cheng, Y. Ma, W. Tseng, H. Chang and W. Hung, *Anal. Chem.*, 2008, **80**, 4845–4852.
- 8 N. Na, M. Zhao, S. Zhang, C. Yang and X. Zhang, *J. Am. Soc. Mass Spectrom.*, 2007, **18**, 1859–1862.
- 9 J. D. Harper, N. A. Charipar, C. C. Mulligan, X. Zhang, R. G. Cooks and Z. Ouyang, *Anal. Chem.*, 2008, **80**, 9097–9104.
- 10 M. Haapala, J. Pi, V. Saarela, V. Arvola, T. Kotiaho, R. A. Ketola, S. Franssila, T. J. Kauppila and R. Kostiaainen, *Anal. Chem.*, 2007, **79**, 7867–7872.
- 11 C. N. McEwen, R. G. McKay and B. S. Larsen, *Anal. Chem.*, 2005, **77**, 7826–7831.
- 12 F. J. Andrade, J. T. Shelley, W. C. Wetzel, M. R. Webb, G. Gamez, S. J. Ray and G. M. Hieftje, *Anal. Chem.*, 2008, **80**, 2646–2653.
- 13 P. Nemes and A. Vertes, *Anal. Chem.*, 2007, **79**, 8098–8106.
- 14 R. Haddad, R. Sparrapan, T. Kotiaho and M. N. Eberlin, *Anal. Chem.*, 2008, **80**, 898–903.
- 15 J. S. Sampson, A. M. Hawkrige and D. C. Muddiman, *J. Am. Soc. Mass Spectrom.*, 2006, **17**, 1712–1716.
- 16 M. J. Ford and G. J. Van-Berkel, *Rapid Commun. Mass Spectrom.*, 2004, **18**, 1303–1309.
- 17 L. V. Ratcliffe, F. J. M. Rutten, D. A. Barrett, T. Whitmore, D. Seymour, C. Greenwood, Y. Aranda-Gonzalvo, S. Robinson and M. McCoustra, *Anal. Chem.*, 2007, **79**, 6094–6101.
- 18 H. Wang, W. Sun, J. Zhang, X. Yang, T. Lin and L. Ding, *Analyst*, 2010, **135**, 688–695.



- 19 K. Jorabchi, M. S. Westphall and L. M. Smith, *J. Am. Soc. Mass Spectrom.*, 2008, **19**, 833–840.
- 20 D. Y. Chang, C. C. Lee and J. Shiea, *Anal. Chem.*, 2002, **74**, 2465–2469.
- 21 M. Li, B. Hu, J. Li, R. Chen, X. Zhang and H. Chen, *Anal. Chem.*, 2009, **81**, 7724–7731.
- 22 H. Chen, A. Wortmann, W. Zhang and R. Zenobi, *Angew. Chem., Int. Ed.*, 2007, **46**, 580–583.
- 23 J. Ding, H. Gu, S. Yang, M. Li, J. Li and H. Chen, *Anal. Chem.*, 2009, **81**, 8632–8638.
- 24 H. Chen, B. Hu and X. Zhang, *Chin. J. Anal. Chem.*, 2010, **38**, 1069–1088.
- 25 W. S. Law, R. Wang, B. Hu, C. Berchtold, L. Meier, H. Chen and R. Zenobi, *Anal. Chem.*, 2010, **82**, 4494–4500.
- 26 H. Chen, A. Venter and R. G. Cooks, *Chem. Commun.*, 2006, 2042–2044.
- 27 H. Chen, S. Yang, M. Li, B. Hu, J. Li and J. Wang, *Angew. Chem., Int. Ed.*, 2010, **49**, 3053–3056.
- 28 H. Chen, J. Lai, Y. Huan, J. Li, X. Zhang, Z. Wang and M. Luo, *Chin. J. Anal. Chem.*, 2007, **35**, 1233–1240.
- 29 H. Chen, G. Gamez and R. Zenobi, *J. Am. Soc. Mass Spectrom.*, 2009, **20**, 1947–1963.
- 30 H. Chen and R. Zenobi, *Nat. Protoc.*, 2008, **3**, 1467–1475.
- 31 N. Na, Y. Xia, Z. Zhu, X. Zhang and R. G. Cooks, *Angew. Chem., Int. Ed.*, 2009, **48**, 2017–2019.
- 32 K. Badjagbo, P. Picard, S. Moore and S. Sauvé, *J. Am. Soc. Mass Spectrom.*, 2009, **20**, 829–836.
- 33 G. Huang, L. Gao, J. Duncan, J. D. Harper, N. L. Sanders, Z. Ouyang and R. G. Cooks, *J. Am. Soc. Mass Spectrom.*, 2010, **21**, 132–135.
- 34 C. Mair, Z. Herman, J. Fedor, M. Lezius and T. D. Mark, *J. Chem. Phys.*, 2003, **118**, 1479–1486.
- 35 J. Brodbelt, C. C. Liou and T. Donovan, *Anal. Chem.*, 1991, **63**, 1205–1209.
- 36 Y. Song and R. G. Cooks, *Rapid Commun. Mass Spectrom.*, 2006, **20**, 3130–3138.
- 37 B. Hu, X. Peng, S. Yang, H. Gu, H. Chen, Y. Huan, T. Zhang and X. Qiao, *J. Am. Soc. Mass Spectrom.*, 2010, **21**, 290–293.
- 38 H. Gu, B. Hu, J. Li, S. Yang, J. Han and H. Chen, *Analyst*, 2010, **135**, 1259–1267.
- 39 H. Gu, S. Yang, J. Li, B. Hu, H. Chen, L. Zhang and Q. Fei, *Analyst*, 2010, **135**, 779–788.
- 40 H. Chen, B. Hu, Y. Hu, Y. Huan, Z. Zhou and X. Qiao, *J. Am. Soc. Mass Spectrom.*, 2009, **20**, 719–722.
- 41 H. Surburg and J. Panten, *Common fragrance and flavor materials*, WILEY-VCH, Weinheim, 2006.
- 42 H. Liang, X. Zhang, S. Chen and Z. Shao, *Chin. J. Anal. Chem.*, 2008, **36**, 1152–1156.
- 43 N. Oyama-Okubo, M. Nakayama and K. Ichimura, *J. Jpn. Soc. Hortic. Sci.*, 2011, **80**, 190–199.
- 44 P. Regal, B. I. Vázquez, C. M. Franco, A. Cepeda and C. Fente, *J. Chromatogr., B*, 2009, **877**, 2457–2464.
- 45 J. F. García-Reyes, A. U. Jackson, A. Molina-Díaz and R. G. Cooks, *Anal. Chem.*, 2009, **81**, 820–829.
- 46 S. Kim, R. Vermeulen, S. Waidyanatha, B. A. Johnson, Q. Lan, N. Rothman, M. T. Smith, L. Zhang, G. Li, M. Shen, S. Yin and S. M. Rappaport, *Carcinogenesis*, 2005, **27**, 772–781.
- 47 S. Waidyanatha, N. Rothman, S. Fustinoni, M. T. Smith, R. B. Hayes, W. Bechtold, M. Dosemeci, L. Guilan, S. Yin and S. M. Rappaport, *Carcinogenesis*, 2000, **22**, 279–286.